Natural Hazards
https://doi.org/10.1007/s11069-021-04963-8

ORIGINAL PAPER

Earthquake-induced landslide prediction using back-propagation type artificial neural network: case study in northern Iran

Ali M. Rajabi[1] · **Mahdi Khodaparast**[2] · **Mostafa Mohammadi**[3]

Received: 24 September 2020 / Accepted: 1 August 2021

Abstract
Landslides can cause extensive damage, particularly those triggered by earthquakes. The current study used back propagation of an artificial neural network (ANN) to conduct risk studies on landslides in the area affected by the Manjil-Rudbar earthquake in Iran in 1990 (M = 7.7). Newmark displacement analysis was used to develop an earthquake-induced landslide hazard map for the blocks representing Chahar-Mahal and Chalkasar near the earthquake epicenter, an area of 309 km^2. The input data included soil cohesion, soil friction angle, unit weight of soil, unit weight of water, distance from hypocenter, slope, and earthquake magnitude as effective parameters for landslide occurrence. The hazard map was compared with an inventory map and other research findings. The results indicated that the landslides predicted by ANN covered 50% of the inventory map of the study area (2088 of 4097 slide cells). The results of the current study suggest that the ANN method is relatively efficient for accurate prediction of landslides.

Keywords Landslide · Earthquake · Newmark displacement · Artificial neural network (ANN) · Back propagation

✉ Mahdi Khodaparast
khodaparast@qom.ac.ir

Ali M. Rajabi
amrajabi@ut.ac.ir; amrajabi@ymail.com

Mostafa Mohammadi
mostafa4p@yahoo.com

[1] Associate Professor, Engineering Geology Department, School of Geology, College of Science, University of Tehran, Tehran, Iran

[2] Associate Professor, Civil Engineering Department, University of Qom, Qom, Iran

[3] Phd Candidate, Civil Engineering Department, University of Qom, Qom, Iran

Published online: 09 August 2021

1 Introduction

Landslides can cause severe damage, especially those caused by earthquakes (Plafker and Galloway 1989; Keefer 1984; Jibson 2007). Much research has been conducted to diagnose and characterize landslides; however, investigation of landslides resulting from earthquakes, particularly in Iran, is in its infancy. A recent method used for the landslide prediction and landslide hazard map preparation is the artificial neural network (ANN). An ANN is a string of robust calculations used to determine the relationship between two datasets. A neural network consists of components as operators on which mathematical calculations are performed to estimate the functions related to the two datasets. This is one of the most important applications of ANNs in engineering, as the network calculates its approximating function by employing a set of input and output data. The back-propagation algorithm in a multilayer ANN is capable of linking the network error at each stage with the weights of the layer (Haykin 2005). Figure 1 is a schematic of the architecture of a multi-layer ANN.

The landslides that accompanied the high-magnitude Manjil-Rudbar earthquake (M = 7.7; 1990) in Iran made it one of the most devastating earthquakes in the history of the country. Several studies have listed the most significant landslides arising from this earthquake. Qualitative and quantitative study of this and other devastating earthquakes (Avaj (M = 6.5; 2002), Firoozabad-e Kojour (M = 6.3; 2004), Kobe (M = 6.9; 1995), Sumatra (M = 9.1; 2004)) could increase knowledge about these natural disasters that would aid in the management of their associated risk.

Attenuation relations have been introduced to estimate the danger caused by earthquakes and assess the expected values of the parameters related to strong earth movement in a particular location at a specific distance from the earthquake hypocenter. Different functional forms have been suggested for these relations. In all of them, the physical governing principles of the earthquake waves are typically integrated with experimental criteria. A broad category of such relations has been presented by various researchers (e.g., Douglas 2001; Stafford et al. 2009). The most common methods for co-seismic slope stability analysis are the semi-static method and Newmark displacement (Newmark 1965). These methods are frequently used along with the geographic information system (GIS) to zone the risk of landslides.

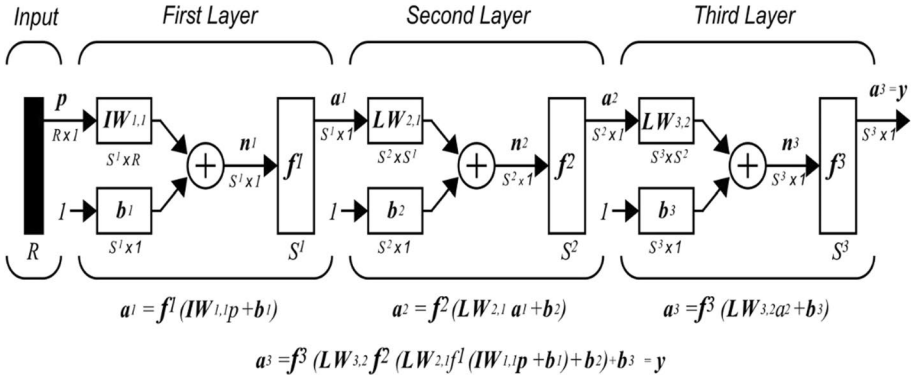

Fig. 1 Architecture of a multi-layer ANN (Sampatrao et al. 2013)

Numerous studies have been conducted in Iran and other countries on landslide hazard zonation using ANN. Pradhan and Lee (2010) studied landslide zonation in the state of the Penang in Malaysia using ANN, remote sensing, and GIS. Other researchers have used GIS, fuzzy logic, and ANN models and have introduced new methods for evaluating landslide risk (Lee and Sambath 2006). Melchiorre et al. (2008) analyzed landslide susceptibility in the southern Alps in Italy using ANN and employed failure analysis to identify unstable zones. Their results demonstrated the efficiency of ANN for zoning landslide risk in a region.

Baharvand and Souri (2015) performed landslide hazard zonation using ANN in the Sepid Dasht region of Lorestan in Iran. Their results showed that 29.85% and 43.52% of the area were in high risk and very-high-risk zones, respectively. Yilmaz (2009) employed ANN, frequency ratios, and logistical regression to zone the landslide risk in Tokat, Turkey. Their results demonstrated that the maps designed by ANN had the highest correlation with actual landslides in the region. Conforty et al. (2014) studied the ability of ANN to predict landslides in North Calabria in Italy and observed that approximately 46% of the study region fell into the high-risk to very-high-risk zones with a consistency of 85%.

Bagheri and Shad (2015) examined the application of ANNs to zoning landslide risk using remotely sensed data and GIS in northern Tehran province. Considering the fault located in this area, the probability of flooding in this area, and the numerous buildings under construction near the lake, the results indicate that landslides would cause significant financial loss and human casualties. Zhang et al. (2012) applied multivariable optimized regression to monitor landslides using satellite imaging. Caniani et al. (2008) used an ANN to design a landslide susceptibility zoning map for Potenza, Italy. Although prediction of landslides using ANN should be important for researchers, few studies have been done on earthquake-induced landslides using this approach. In addition, most studies on landslide prediction using ANNs have not considered the earthquake factor.

Zhou et al. (2018) studied landslide susceptibility for Longju in the Three Gorges Reservoir area in China by applying machine learning methods in order to develop effective risk prevention and mitigation strategies. Two machine learning models (support vector machine (SVM) and artificial neural network) and a multivariate statistical model (logistic regression) were applied for landslide susceptibility modeling. The results showed that the machine learning models outperformed the multivariate statistical model and that the SVM model was found to be ideal for the case study area.

Li et al. (2017) investigated the prediction of landslide zones using seismic amplitude in Liwan gas field in the northern part of the South China Sea based on statistical analysis results. The results indicated that the areas have a high potential for shallow landslides on slopes exceeding 15° when the thickness of the loose sediment exceeds 8 m. Chen et al. (2017) studied on the prediction of landslide susceptibility using an adaptive neuro-fuzzy inference system combined with frequency ratios, a generalized additive model, and SVM techniques. The results showed that all three models had good prediction capabilities.

Some probabilistic methods have been used to assess the earthquake-induced landslide hazard. Rathje and Saygili (2011) used pseudo-probabilistic and fully probabilistic approaches to predict expected sliding displacement. The results showed that pseudo-probabilistic analysis provided non-conservative estimates of sliding displacement in most cases. Del Gaudio et al. (2003) introduced a type of time-probabilistic method for evaluation of seismically induced landslide hazards. This approach was applied to an area in southern Italy and showed that the introduction of the time factor significantly modified the representation of the spatial hazard and allowed evaluation of the relevance of seismicity as a landslide triggering agent.

Rajabi et al. (2013) studied co-seismic landslide hazards in Iran using the time-probabilistic approach. They used the method developed by Del Gaudio et al. (2003) to estimate co-seismic landslide hazards based on critical acceleration (A_c), which shows the minimum slope resistance required to limit the probability of seismic triggering of a landslide within a fixed value. Using this approach, occurrence probabilities for different levels of seismic shaking were measured. The application of this method to Iran indicated that the highest levels of seismic-landslide hazard is in the northern part of the country, which is exposed to the effects of the less frequent, but more energetic, seismic activity of the Alborz zone. Here A_c values of up to 0.1 g are required to contain the probability of occurrence of seismically induced landslides within the limits (10% in 50 years) considered acceptable in seismic risk assessment for ordinary building damage.

Refice and Capolongo (2002) supplied an earthquake-induced landslide hazard map that considered uncertainty originating from spatial variability of geological, geotechnical, geomorphological, and seismological parameters based on the simplified Newmark slope stability model. They implemented uncertainty as input data using probability distribution functions. They showed good performance for realistic landslides in southern Italy. Mankelow and Murphy (1998) showed that modeling the uncertainty as a probability distribution function will improve the prediction capabilities of Newmark's model. The authors propagated the uncertainty using the model equations and determined the statistical parameters of the final probability distribution for the Newmark displacement.

Lee and Evangelista (2006) studied earthquake-induced landslide-susceptibility mapping in Baguio in the Philippines using an ANN. They showed that the susceptibility map obtained using back propagation had an accuracy of 93.2%. Liu et al. (2020) studied landslide displacement prediction using multi-source data fusion and sensitivity states. They reported that the proposed model outperformed the traditional prediction models with low error. Bui et al. (2020) compared conventional machine-learning and deep-learning neural networks for predicting the occurrence of landslides. Their results showed that the deep-learning neural network model outperformed the conventional machine-learning method.

The Manjil region has a history of severe earthquakes and slippage hazards caused by earthquakes. Because the studies conducted thus far on this area have been limited to deterministic research, in the current study, an attempt was made to investigate and predict landslides in this region using an ANN method. The present research used a back-propagation neural network algorithm and GIS. It took into account significant factors affecting earthquake-induced landslides when predicting landslides in the Manjil region. The accuracy of this method in predicting locations susceptible to landslides then was evaluated.

2 Study area

The study area and geological setting experienced many landslides that were triggered by the Manjil-Rudbar earthquake. These resulted in the closure of mountain roads and some parts of the main Qazvin-Rasht highway. The study area is located at 49°30' and 49°45' E longitude and 35°45′00″ and 35°52′30″ N latitude and covers an area of 309.30 km^2 (Fig. 2a). The nearest and farthest points were 20.64 and 42.43 km from the Manjil-Rudbar earthquake epicenter, respectively. The epicenter of the earthquake was 20.64 km from the northwest corner of the study area.

There is a diversity of geological materials in the study area ranging from Precambrian metamorphic rock to Quaternary sediment. In most of the Alborz zone, red

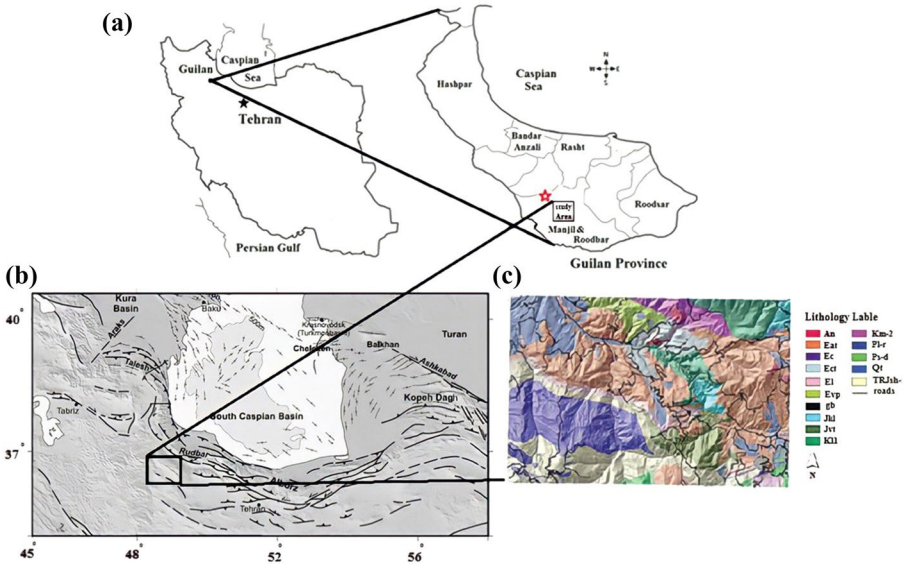

Fig. 2 Geological map and generalized tectonic map of south Caspian Sea and surrounding region showing major active faults. The red star denotes the epicenter of the Manjil-Rudbar earthquake (adapted from Jackson et al. 2002)

sandstone overlies the Infra-Cambrian rock and no changes have occurred in the Paleozoic sedimentation or geological characteristics. Because of two instances of uplift in these areas, there is no Silurian or carboniferous sediment. Triassic rock with erosional discontinuities overlies the Permian strata.

The sandstone, shale, and conglomerates of the Shemshak Formation, which have formed on the eroded surface, exhibit very different thicknesses due to their many protrusions and dents. The Lar Formation (limestone; upper-middle Jurassic) has covered the Shemshak Formation in its isoclinal fold. Cretaceous deposits of limestone, marl, and volcanic lava, as well as Paleogenic rock that include conglomerates, limestone nummulites, and Karaj Formation rock are the most frequent geological outcrops in the area. Quaternary sediment in the inter-mountainous basins, alluvial terraces, and alluvial fans with erosional discontinuities has covered the ancient sediment. Figure 2 shows that the lithology of the region mainly comprises thick and medium limestone, gray limestone, tuff, andesite tuff, and volcanic basaltic stone located to the west, center, east, northwest, and northeast of the region, respectively. Figure 2b presents the geological units of the study area. The lithology definitions are shown in Table 1.

The Manjil-Rudbar earthquake is one of three large-magnitude events to have occurred in this part of the Alborz in recorded history. The earthquake is the largest instrumentally recorded event in the Alborz Mountains in northern Iran and is associated with a range-parallel left-lateral strike-slip surface rupture of 180 km.

Iran is situated over the Alpide Himalayan seismic belt and is one of the most seismically active areas of the world. One important features of the Iranian plate is young tectonic movement. In this region, faults movements do not follow a logical process. In the Alborz region, horizontal movement can be observed along the faults in addition to

Table 1 Lithology label definitions (Fig. 2b)

Geological formation	Label	ɣ* (g/cm^3)	*C*' (kPa)			φ'(deg)			m
			Min	Max	SD	Min	Max	SD	
Andesite tuff, dacite	Ect	2.6	15	25	3.15	12	23	3.59	1
Volcanic dacite stone	Dc-An	2.6	120	160	13.47	34	54	6.75	1
Thick and medium lime	Plr	2.5	20	50	9.9	20	26	2.23	1
Shale and sandstone	Psd	2.2	20	40	6.8	20	25	1.82	1
Andesite tuff, dacite	Evp	2.2	15	25	3.35	14	19	1.78	1
Basaltic tuff	Eat	2.6	23	40	5.7	14	38	6.97	1
Volcanic basaltic stone	Jvt	2.6	20	100	26.65	20	32	3.76	1
Shale and sandstone	TRjs	2.4	60	120	20.6	34	42	2.50	1
Fossiliferous lime	Jkl	2.5	250	340	28.7	31	50	5.02	1
Lime stone	Kll	2.7	240	320	30.3	32	51	6.96	1
Weathered soil and marl	K2m	2.7	25	40	5.8	18	24	2.09	1
Gabbro	Gb	2.8	220	270	16.32	40	60	5.18	1
Conglomerate	Ec	2.5	50	80	9.61	34	45	3.73	1
Gray limestone and tuff	El	2.5	75	120	14.39	42	46	1.51	1
Recent sediment	Qt	1.96	17	35	6.4	25	45	6.71	1

vertical movement, which is the reason for the turbulent deformations. The most important of these deformations in the central Alborz region became apparent after the 1990 Manjil-Rudbar earthquake.

The complex tectonics of the central Alborz and the existence of Gilan to the southwest of the Caspian Sea means that this area has a high potential for seismic activity in Iran. The reason why this area is so seismically hazardous is because of the changes in tectonic behavior in the semi-oceanic crust at the bottom of the Caspian Sea (Ghodrati and Amrei 2008). As shown in Fig. 2c, there are many active faults in this area that increase concerns and have led to implementation of this study. The main faults in this region are the Manjil-Rudbar, North Alborz, and Khazar with lengths of 152, 300, and 600 km, respectively. The faults in this area have a high potential for seismic activity and it is expected that tectonic movement will cause destruction along the active faults.

2.1 Geodynamic and tectonic characteristics of study area

The active tectonics of the study area are affected by major faults having a northwest trend. This is a broad brittle shear zone defined by nearly parallel fault sections. Geomorphic investigation along the Rudbar, Manjil, and Clichomus faults provide evidence of left-sided displacement by alluvial fans, indicating Quaternary fault activity. The Rudbar, Manjil, Klischum and Kashachal (Jirandeh) faults belong to a structure located on the southern border of the western Alborz at 48.20° to 50.30° east longitude.

2.2 Manjil-Rudbar earthquake

The Manjil-Rudbar earthquake (Ms 7.7) occurred on 20 June 1990 in a densely populated area of northern Iran (Gilan and Zanjan provinces) along a previously unknown

complex of inverted faults that are now known as the Baklor-Kabateh-Zardgoli fault. The Baklor section lies to the west, the Kabateh section in the center, and the Zard-Goli section to the east. They are generally arranged in an internal stair system in a WNW direction (Berberian and Walker, 2010). An earthquake rupture dip was identified that is nearly vertical (Berberian and Walker, 2010). Earthquake focal analysis shows a left-ward mechanism for the main shock. Although the structural style of the region has been affected by reverse faulting, the focal mechanisms of subsequent seismic events (for the 11 largest aftershocks around4.6) indicate a net left-slip motion (Gao and Wallace, 1995).

3 Landslides induced by Manjil-Rudbar earthquake

The Manjil-Rudbar earthquake triggered hundreds of landslides, some of which blocked mountain roads. Many houses, orchards, farms and water supply systems were destroyed in the earthquake and more than 200 people lost their lives (Komakpanah and Hafezi-moghaddas 1993). Different types of landslides, including coherent slides and rock falls, were reported in the region, but these were not recorded until months after the earthquake. As a result, the effects of the small landslides had been erased and only the larger landslides were reported. Mahdavifar (2006) identified 51 landslides resulting from the Manjil-Rudbar earthquake through field observation, by extracting information from the literature, and by studying aerial images of a region of 309 km^2 that included Chahar-Mahal and Chalkasar (Fig. 3).

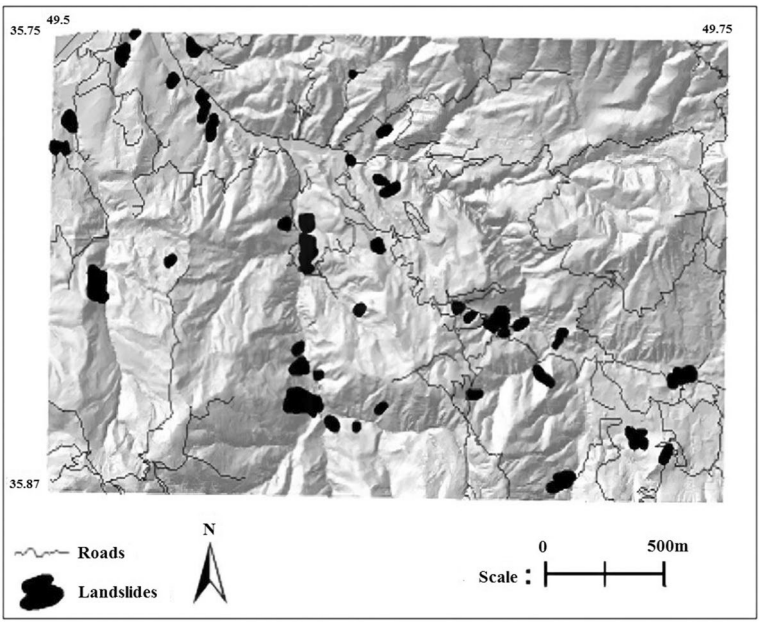

Fig. 3 Inventory map of landslides caused by Manjil-Rudbar earthquake in study area (Mahdavifar 2006)

4 Materials and methods

An ANN can compute and map a specific problem using a set of data from one multivariate space of information to another. The back-propagation training algorithm, as the most common ANN method, was used in the present study. This method is trained using a set of associated input and output values and aims to build a model of the data-generating process so that the network can generalize and predict outputs from inputs. An ANN learns by regulating the weights between the neurons in response to errors between the actual output values and target output values. At the end of the training phase, the neural network will provide a model that should be able to predict a target value from a given input value (Garrett 1994).

The present research considered seven effective factors for zoning the risk of occurrence of earthquake-induced landslides in the study area. These are the friction angle, cohesion of the soil, unit weight of the soil, unit weight of the water, distance from the hypocenter, slope, and magnitude of the earthquake. The Newmark displacement criterion was used to predict a landslide; thus, the factors that were selected as input data to the neural network were those that affected the Newmark value.

Local factors can limit the accuracy of the results in specific cases. Jibson and Harp (2002) reported that topographic amplification caused high PGA values and consequent rock falls. However, in the present study a (acceleration) was assumed to be constant and R (distance from hypocenter) altered the effect of acceleration in different points; thus, topography amplification was a limitation of this research that was not considered.

Bozzano et al. (2008) reported that amplification effects were primarily due to the shallow basin-like structure. However, in this research, assumptions that have been described in the literature and which were close to the actual system of the study area were used for simplification. Heavy rainfall in the study area has caused a high groundwater level and the soil is saturated; thus, it was assumed that the study was implemented during a high rainfall season. The soil cohesion and internal friction angle were effective factors for landslides in the study area and were determined from field studies and RocLab software according to the Hoek and Brown (1980) criterion. In the present study, landslides were predicted using the available conditions and data.

In the study region, landslides primarily occur on rocky slopes and are usually discrete. Information about the cohesion layers and internal friction angle was obtained by preparing a geological map of the region through field studies and by determination of the geomechanical properties of the geological units and then digitizing the results. The geotechnical parameters required to determine the safety factor, including the internal friction angle and cohesion, were estimated according to Hoek and Brown (1980) using RocLab software and GSI based on lithological similarity and discontinuities (Table 1). RocLab was used to estimate the shear strength parameters for each geological unit. In some cases, the validity of the results was verified with laboratory and field tests.

The choice of the factors relates to their effect on landslides induced by earthquakes and other data constraints. The unit weight of the soil was calculated for each geological unit. The unit weight of the water and the magnitude of the Manjil-Rudbar earthquake were held constant for each point (9.81 m/s^2 and 7.7 M_w on the Richter scale, respectively). The distance from the hypocenter and the slopes of the different cells were derived from a digital elevation model. Each of these parameters was divided into different intervals in the GIS.

The features of each map were determined first when using the effective factors for zoning the risk of landslides. Each factor was divided into cells of the same dimension

and then converted into points to assess the effect of significant factors on the occurrence of landslides in each cell using GIS. All of the maps were compatible at a certain scale. The features of each point contained the integer values of each cell after conversion into points. The size of each cell was 1×1 m^2. After conversion, 400 points were selected for ANN training and validation with the aim of determining the objective function while holding the two factors constant. The points selected covered diverse extremes of other features. The back-propagation algorithm was used to predict the risk of landslide. Of the 400 points, 320 were used for training and 80 for validation.

The input data selection depends on the output factor used for prediction of landslides induced by an earthquake. In accordance with Jibson et al. (2000), all factors used either directly or indirectly affected the Newmark displacement (see Eq. (1)). The friction angle, cohesion, and the unit weight of the soil were the geotechnical parameters of the study area, and the water condition was an environmental factor that would affect the safety factor used for calculating the critical acceleration. According to Mahdavifar (2006), the distance from the hypocenter, the slope, and the magnitude of the earthquake directly affect the Arias intensity. This indicates that all factors used directly affected the Newmark displacement.

The 400 data points used were chosen such that the majority of the data of the region was covered. Of the 400 data points, 285 were selected from landslide cells and 115 from non-event cells. The selection of input data was random, but the maximum, minimum and repeat data values were considered for each factor. The maximum and minimum values of the geotechnical factors are listed in Table 1. The output data used for network learning were derived by Newmark displacement, which was estimated for each point (Mahdavifar 2006) as:

$$\mathrm{Log}D_N = 1.087 \log I_a - 7.176 + 1.398 \pm 0.397 \tag{1}$$

where D_N is the Newark displacement, a_c is the critical acceleration, and I_a is the Arias intensity. To obtain the Newmark displacement for each point, the Arias intensity must be computed (Mahdavifar 2006) as:

$$\mathrm{Log}I_a = -3.880 + 0.810M - \log R - 0.002R \tag{2}$$

where M is the earthquake magnitude and R is the distance from the hypocenter.

Determination of the threshold acceleration depends on the safety factor of each unit. In the Newmark method, dynamic slope stability depends on its static stability. A simple limit equilibrium model was developed for analysis at regional scale that was based on planar failure, as recommended by Jibson et al. (2000). The safety factor can be computed as:

$$Fs = \frac{c'}{\gamma t sin\alpha} + \frac{\tan\varphi'}{\tan\alpha} - \frac{m\gamma_w \tan\varphi'}{\gamma \tan\alpha} \tag{3}$$

where c' is soil cohesion, φ' is the soil friction angle, γ and γ_w are the unit weight of the soil and water, respectively, α is the slope, and m is the proportion of slab thickness that is saturated. In the study area, parameter m was assumed to be equal to 1 because of the high rate of precipitation, which causes ground saturation in the region; thus, the results would become more conservative. Also, field investigation indicates that most of the landslides were shallow; thus, a depth of 3 m was considered.

By combining the safety factor of each cell with its slope, which shows sensitivity to landslides caused by earthquakes in the cell, the threshold acceleration can be obtained using the Newmark method as:

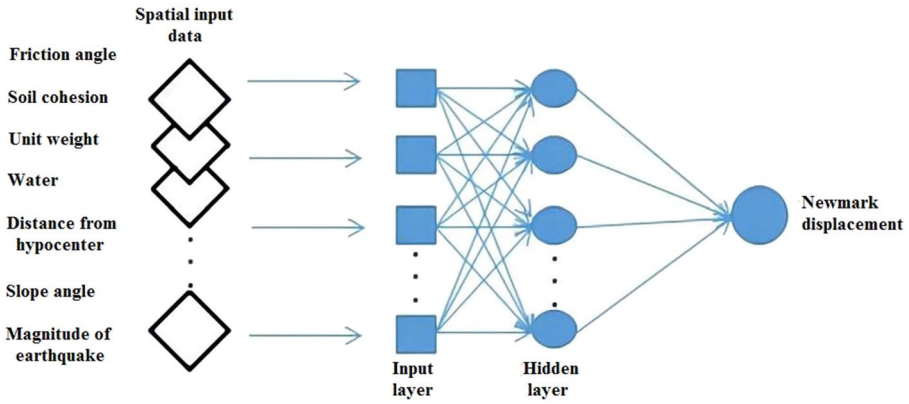

Fig. 4 Architecture of ANN designed to predict Newmark displacement

Table 2 Percentage of landslides predicted in region

Type of landslide	Number of predicted cells	Landslide area (km^2)	Ratio of predicted cells to whole area (%)
Coherent	61,461	55.31	17.9
Rock fall	9431	8.49	2.74
Total landslide area	70,892	63.80	20.64

$$a_c = \left(F_s - 1\right) g sin\alpha \tag{4}$$

where a_c is the critical acceleration, F_s is the safety factor, and g is gravity acceleration.

The Newmark displacement was obtained after computing the Arias intensity and threshold acceleration for each cell. These results were used as output data for the ANN. As mentioned, 80% of the input data was used to train the network and the remaining 20% was used for validation. To develop the algorithm for prediction, one hidden middle layer with ten neurons was chosen. The architecture of this network is shown in Fig. 4.

After preparation of the ANN, the Newmark displacement for all cells was predicted and all data gathered from the ANN were transferred to the GIS to prepare the earthquake-induced landslide hazard map. The network consists of three layers. The first layer is the input layer, where the nodes are the elements of a feature vector. The second layer is the internal or "hidden" layer. The third layer is the output layer and represents the output data. Each node in the hidden layer is interconnected to nodes in both the preceding and following layers through weighted connections.

5 Results and discussion

The final hazard map of landslides predicted by ANN is shown in Fig. 6. Using the input data and architecture of the ANN, 70,892 landslide cells were predicted for the region (61,461 sliding cells for coherent landslides and 9,431 rock falls; 17.9% and 2.74%, respectively; Table 2). Distinguishing the coherent and disrupted landslides was based on the

Newmark model, which provides an estimate of permanent displacement (D_N) along a potential sliding surface and assumes that the exceedance of critical values of D_N defines conditions that trigger landslides. According to Wilson and Keefer (1985), the critical values for coherent and disrupted landslides are 10 cm and 2 cm, respectively.

The map produced by ANN was compared with the inventory map of the landslides to determine the accuracy of the method. Figure 5 shows the landslide hazard map predicted by ANN overlapped by the inventory.

Gee (1992) developed the quantified sum index (QS) to assess the degree of efficiency of zonation maps when comparing predictive landslide maps with other methods. This variable is based on data distribution around the mean. According to Gee, QS will increase as the accuracy of the zonation map increases. To compute QS, a density ratio variable must be determined as:

$$Dr = \frac{L\%}{A\%} \tag{5}$$

where D_r is the density ratio, $L\%$ is the percentage of total landslides in the zone considered, and $A\%$ is the percentage of area occupied by the zone.

Gee (1992) found that a value of $D_r = 1$ means the landslide density in the considered zone equals the average density of landslides and $D_r > 1$ and $D_r < 1$ denote higher or lower densities, respectively, compared to the average density. After computation of D_r for each group, the value of QS can be obtained as:

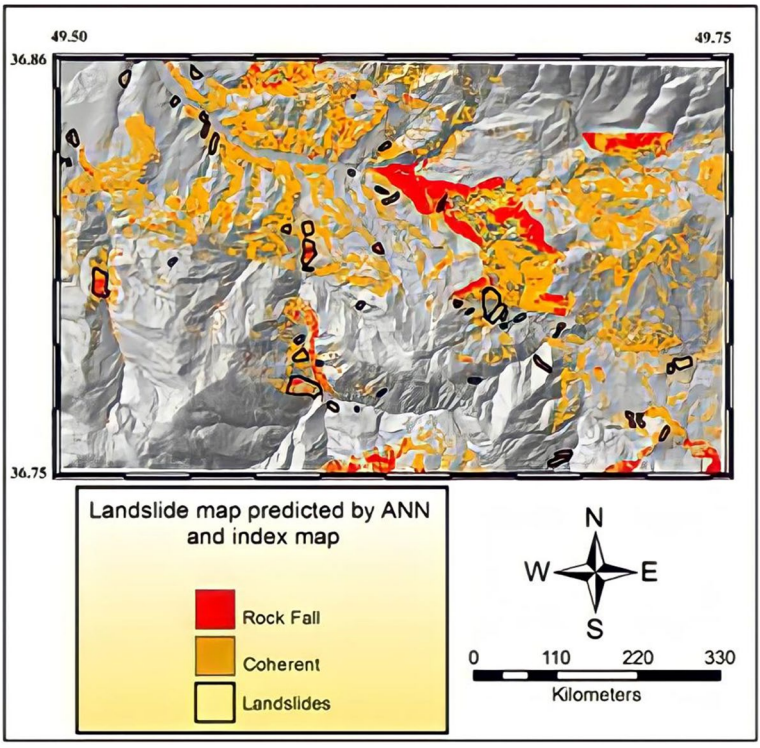

Fig. 5 Comparison of landslide hazard map predicted by ANN and inventory map

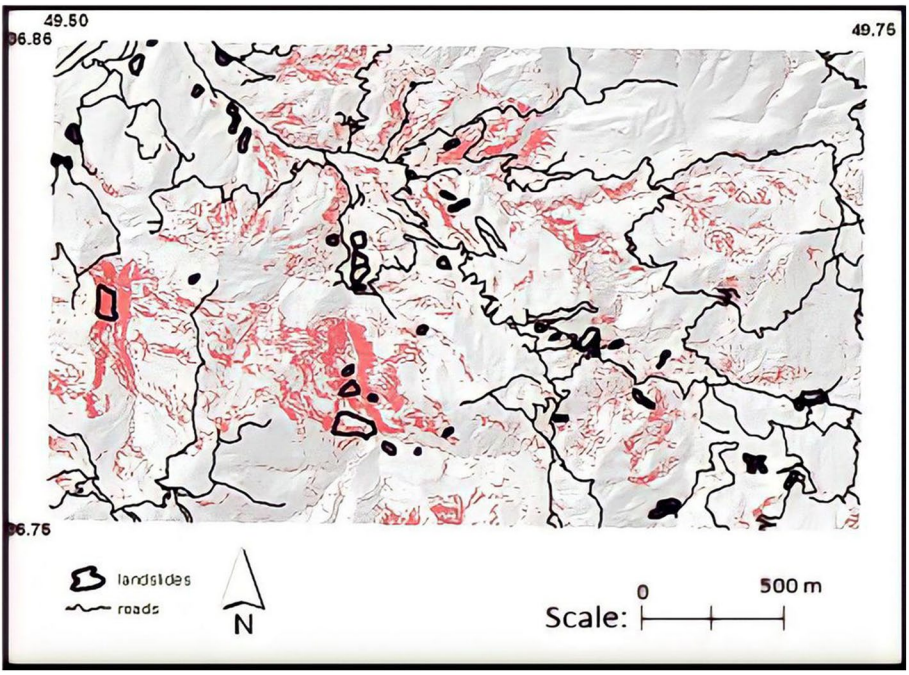

Fig. 6 Landslide map predicted by deterministic method (Mahdavifar 2006)

Table 3 QS (quantified sum index) and D_r (landslide density ratio) of method

Method	Group	D_r	QS
Deterministic (Mahdavifar 2006)	1	2.09	59.4
	2	0.46	
This study	1	2.47	109.69
	2	0.739	

$$\mathrm{QS} = \sum_{i=1}^{n} (Dr_i - 1)^2 \times A_i\% \tag{6}$$

where Dr_i and A_i are the density ratio and percentage of area of each zone, respectively, and n is the number of zones on the map. Using this method, the map derived using ANN was divided into a high risk zone (predicted to have landslides) and a low risk zone (predicted to have no landslides). Mahdavifar (2006) prepared an earthquake-induced landslide hazard map for this region using a deterministic approach (Fig. 6). In both methods, the same input data were used for landslide risk assessment.

Table 3 compares the results of the ANN method with the deterministic method. In both approaches, the maps were divided to a high-risk group (1) and a low risk group (2). The computed QS values indicate that the ANN method (109.69) better predicted landslides than the deterministic method which uses a constant variable (59.40). The safety factor and hazard maps obtained using the deterministic method were not able to directly take into account uncertainty. In the probabilistic method using Newmark analysis, some of the

uncertainty caused by geological, geomorphological, and seismic data was imported into the model through statistical distribution functions.

The statistical index and the mean error (ME) were used to evaluate the selected back-propagation network as:

$$ME = \frac{1}{n}\left(\sum_{i}^{n}(y - y_i\right) \tag{7}$$

where y is the Newmark displacement measured under real conditions and y_i is the Newmark displacement from the back-propagation method. An ME of 35% was obtained for the back-propagation method. These results indicate that the high rate of uncertainty had a negative effect on the network efficiency and accuracy of this method. Figure 7 presents the overlap of the predicted results and real conditions. As can be seen from the figure, the predicted and real results are fairly consistent. In this graph, the Newmark displacement for non-sliding, rockfall, and coherent sliding was assumed to be 1, 2, and 3, respectively.

According to the results of the present study and their comparison with the deterministic method used in the area for landslide prediction (Mahdavifar 2006), the method used in this study performed better for predicting a landslide hazard. However, comparison of the landslide inventory map and the map obtained by the ANN method indicates that the latter method predicted more points as slip-prone areas. In the inventory map, many landslides were removed because their slopes were slight. These landslides were considered to be caused by displacement due to liquefaction, which cannot be evaluated by the Newmark (1965) approach used in this study. Also, the presence of uncertainty in these methods relating to the assumptions and simplifications that were used for modeling affected the accuracy of the method.

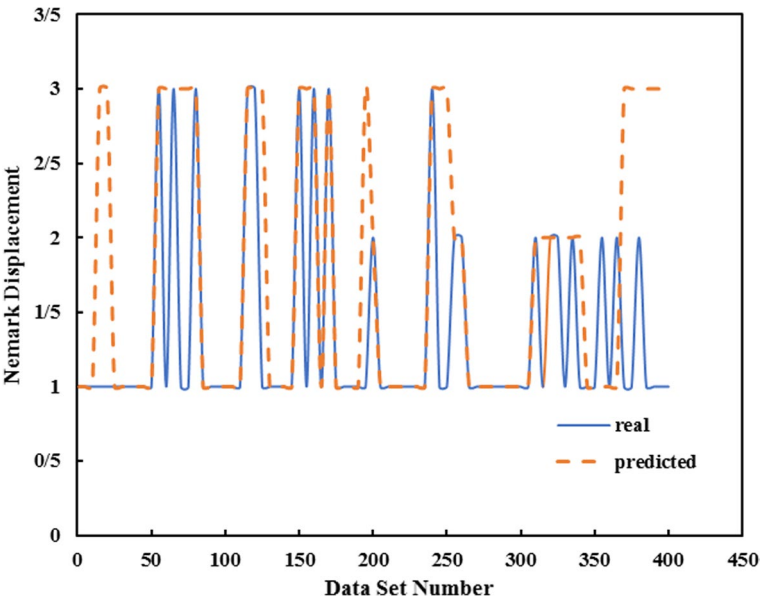

Fig. 7 Overlap of predicted and real conditions

Due to the scale of the study area, a large number of the landslides were small and could not be mapped and, thus, have not been included in the inventory map. Also, because the study was point-to-point, each point with slip potential has been shown as a slip location, although they do not have significant range. It should be noted that the Q factor can be suitable for use in this type of study (Jibson and Harp 2002). A comparison of the results of the research method and the deterministic method indicate that the ANN method exhibited many possible landslide points that have a much better overlap with real landslides. This can be considered to be a positive result for this method.

6 Conclusions

One of the most important effects of the Manjil-Rudbar earthquake (M = 7.7; 1990) was the occurrence of numerous landslides induced by the earthquake. In this research, an artificial neural network (ANN) was used to predict landslides induced by the Manjil-Rudbar earthquake. A back-propagation algorithm was used to predict the earthquake-induced landslides in a study area of about 309 km^2 that included the blocks representing Chahar-Mahal and Chalkasar near the epicenter.

Seven types of input data (soil cohesion, soil friction angle, specific weight of soil, specific weight of water, distance from hypocenter, slope, and magnitude of the earthquake) were considered. For generation and training of the algorithm, of the 400 data points chosen, 285 were from landslide cells and 115 were from non-event cells. The results obtained by the ANN algorithm were converted into a map using GIS technique. The map showed that ANN better predicted the landslides than did the deterministic method. A previously defined quantifier variable (QS) was used to evaluate the degree of efficiency of the hazard map and chose the ANN method (106.69) over the deterministic method (59.4).

An ME of 35% was obtained for the back-propagation method. This value indicates a negative effect of uncertainty on network efficiency. However, the neural network method based on Newmark analysis allowed some of the uncertainty arising from geological, geomorphological, and seismic data to enter the model. The application of this method in the study area showed that it was more effective for predicting risk areas than the deterministic method, although a number of problems remained unresolved due to the geological complexity of the area.

Acknowledgements The authors would like to thank Mr. Edalat, PhD candidate, for his insightful comments and useful suggestions.

Declarations

Conflict of interest The author declares that there is no conflict of interest.

References

Bagheri A, Shad R (2015) Application of artificial neural network in landslide hazard zonation by remote sensing and GIS, International Conference of Civil Engineering and Architecture and urban infrastructure, Tabriz, Iran.

Baharvand S, Souri S (2015) Landslide susceptibility zonation with artificial neural network, case study: Sepid dasht, Lorestan, remote sensing and GIS publication, (In Persian).

Berberian M, Walker R (2010) The Rudbār Mw 7.3 earthquake of 1990 June 20; seismotectonics, coseismic and geomorphic displacements, and historic earthquakes of the western 'High-Alborz' Iran. Geophys J Int 182(3):1577–1602

Bozzano F, Lenti L, Martino S, Paciello A, Scarascia Mugnozza G (2008) Self-excitation process due to local seismicamplification responsible for the reactivation of the Salcito landslide (Italy) on 31 October 2002. J Geophys Res Solid Earth113(B10)

Bui TT, Tsangaratos P, Nguyen V, Liem NV, Trinh PT (2020) Comparing the prediction performance of a Deep Learning Neural Network model with conventional machine learning models in landslide susceptibility assessment. CATENA, 188

Caniani D, Pascale S, Sdao F, Sole A (2008) Neural networks and landslide susceptibility: a case study of the urban area of Potenza. Nat Hazards 45(1):55–72

Chen W, Pourghasemi H, Panahi M, Kornejady A, Wang J, Xie X, Cao S (2017) Spatial prediction of landslide susceptibility using an adaptive neuro-fuzzy inference system combined with frequency ratio, generalized additive model, and support vector machine techniques. Geomorphology 297:69–85

Conforti M, Pascale S, Robustelli G, Sdao F (2014) Evaluation of prediction capability of the artificial neural networks for mapping landslide susceptibility in the Turbolo River catchment (Northern Calabria, Italy). CATENA 113:236–250

Del Gaudio V, Pierri P, Wasowski J (2003) An Approach to time-probabilistic evaluation of seismically induced landslide hazard. Bull Seismol Soc Am 93(2):557–569

Douglas J (2001) A comprehensive worldwide summary of strong-motion attenuation relationships for peak ground acceleration and spectral ordinates (1969–2000), Imperial College of Science, Technology and Medicine, Civil Engineering Department.

Gao L, Wallace TC (1995) The 1990 Rudbar-Tarom Iranian earthquake sequence: evidence for slip partitioning. Journal of Geophysical Research Solid Earth 100(B8):15317–15332

Garrett J (1994) Where and why artificial neural networks are applicable in civil engineering [J]. J Compute Civil Eng 8:129–130

Gee M D (1992) Classification of landslide hazard zonation methods and a test of predictive capability. Proceeding of 6th International Symposium on Landslides, Christchurch, New Zealand, 2:947–952.

Ghodrati Amiri G, Razavian Amrei SA, (2008) Seismic hazard assessment of gilan province including manjil in Iran. The 14th World Conference on Earthquake Engineering October 12–17, Beijing, China.

Harp EL, Jibson WR (2002) Anomalous concentrations of seismically triggered rock falls in pacoima canyon: are they caused by highly susceptible slopes or local amplification of seismic shaking? Bull Seismol Soc Am 92(8):3180–3189

Haykin S (2005) Neural networks a comprehensive foundation. McMaster University Hamilton, Ontario

Hoek E, Brown E (1980) Empirical Strength criterion for rock masses. J Geotech Eng Div ASCE 106(GT9):1013–1035

Hoek E, Brown ET (1980) Empirical strength criterion for rocks masses. J Geotech Eng Devis. https://doi.org/10.1061/AJGEB6.0001029

Jackson J, Priestly K, Allen M, Berberian M (2002) Active tectonics of South Caspian Basin. Geophysics J Int 148(2):214–245

Jibson RW (2007) Regression models for estimating coseismic landslide displacement. Eng Geol 91:912–918

Jibson RW, Harp EL, Michael JA (2000) A method for producing digital probabilistic seismic landslide hazard maps. Eng Geol 58:271–289

Keefer DK (1984) Landslides caused by earthquakes. Geol Soc Am Bull 95:406–421

Komakpanah A, Hafezimoghaddas N (1993) landslide hazard zonation in Iran. Identifying and mapping of landslide triggered by Manjil earthquake. Int Inst Earthq Eng Earthq Sociol.

Lee S, Evangelista DG (2006) Earthquake-induced landslide-susceptibility mapping using anartificial neural networkS. Nat Hazards Earth Syst Sci 6:687–695

Lee S, Sambath T (2006) Landslide susceptibility mapping in the Damrei Romel area, Cambodia using frequency ratio and logistic regression models. Environ Geol 50(6):847–856

Li X, Liu B, Liu L, Zheng J, Zhou S, Zhou Q (2017) Prediction for potential landslide zones using seismic amplitude in Liwan gas field, northern South China Sea. J Ocean Univ China 16(6):1035–1042

Liu Y, Xu C, Huang B, Ren X, Liu C, Hu B, Chen Z (2020) Landslide displacement prediction based on multi-source data fusion and sensitivity states. Eng Geol. https://doi.org/10.1016/j.enggeo.2020.105608

Mahdavifar M R (2006) evaluation analysis and design of risk management system of landslide induce by earthquake in Iran, PhD Thesis, Institute of Earthquake Engineering Seismology.

Mankelow JM, Murphy W (1998) Using GIS in the probabilistic assessment of earthquake triggered landslides hazards. J Earthquake Eng 2(4):593–623

Melchiorre C, Matteucci M, Azzoni A, Zanchi A (2008) Artificial neural networks and cluster analysis in landslide susceptibility zonation. Geomorphology 94(3):379–400

Newmark NM (1965) Effects of earthquakes on dams and embankments. Geotechnique 15:139–160

Plafker G, Galloway JP (1989) Lessons learned from the Loma Prieta, California earthquake of October 17, and extracted specific data sets from them. US Geol Surv Circ 1045:1989

Pradhan B, Lee S (2010) Delineation of landslide hazard areas on penang island, Malaysia, by using frequency ratio, logistic regression, and Artificial neural network models. Environ Earth Sci 60(5):1037–1054

Rajabi AM, Khamehchiyan M, Mahdavifar MR, Del Gaudio V, Capolongo D (2013) A time probabilistic approach to seismic landslide hazard estimates in Iran. Soil Dyn Earthq Eng 48:25–34

Rathje EM, Saygili G (2011) Pseudo-Probabilistic versus Fully Probabilistic Estimates of Sliding Displacements of Slopes. J Geotech Geo Environ Eng ASCE 137(3):208–221

Refice A, Capolongo D (2002) Probabilistic modeling of uncertainties in earthquake-induced landslide hazard assessment. Comput Geosci 28:735–749

Sampatrao L, Pinjare E, Kumar H (2013) Implementation of Artificial Neural Network Architecture for Image Compression Using CSD Multiplier. Proceedings of International Conference on Emerging Research in Computing, Information, Communication and Applications, P581–587, August 2013, Bangalore India.

Stafford PJ, Berrill JB, Pettinga JR (2009) New predictive equations for Arias intensity from crustal earthquakes in New Zealand. J Seismolog 13(1):31–52

Wilson RC, Keefer DK (1985) Predicting aerial limits of earthquake-induced land sliding. In, J.I. Ziony (ed.), Evaluating earthquake hazards in the Los Angeles region-An Earth-Science perspective, USGS Professional paper 1360, pp. 316–345.

Yilmaz I (2009) Landslide susceptibility mapping using frequency ratio, logistic regression, artificial neural networks and their comparison: a case study from Kat landslides (Tokat-Turkey). Comput Geosci 35(6):1125–1138

Zhang W, Wang W, Wu F (2012) The application of multi-variable optimum regression analysis to remote sensing imageries in monitoring landslide disaster. Energy Procedia 16:190–196

Zhou C, Yina K, Caoa Y (2018) Landslide susceptibility modeling applying machine learning methods: a case study from Longju in the Three Gorges Reservoir area, China. Comput Geosci 112:23–37